Polymorphism of Cellulose I Family: Reinvestigation of Cellulose IV I

ARTICLE *in* BIOMACROMOLECULES · JULY 2004

Impact Factor: 5.75 · DOI: 10.1021/bm0345357 · Source: PubMed

Polymorphism of Cellulose I Family: Reinvestigation of Cellulose IV_I

Masahisa Wada,[†,*] Laurent Heux,[‡] and Junji Sugiyama[§]

Department of Biomaterials Science, Graduate School of Agricultural and Life Sciences, The University of Tokyo, Yayoi 1-1-1, Bunkyo-ku, Tokyo 113-8657, Japan, Centre de Recherches sur les Macromolécules Végétales (Affiliated with Joseph Fourier University of Grenoble), C.N.R.S. B.P. 53, 38401, Grenoble Cedex 9, France, and Research Institute for Sustainable Humanosphere, Kyoto University, Kyoto 611-0011, Japan

Received December 18, 2003; Revised Manuscript Received April 7, 2004

Polymorphs of cellulose I, III_I, and IV_I have been investigated by X-ray diffraction, FT-IR, and solid-state ^{13}C NMR spectroscopy. Highly crystalline cellulose III_I samples were prepared by treating cellulose samples in supercritical ammonia at 140 °C for 1 h, and conventional cellulose III_I samples were prepared by liquid ammonia treatment. The cellulose IV_I sample of highest crystallinity was that prepared from *Cladophora* cellulose III_I in supercritical ammonia, followed by the sample treated in glycerol at 260 °C for 0.5 h, whereas the lowest crystallinity was observed in ramie cellulose prepared by conventional liquid ammonia treatment followed by glycerol annealing. In general, the perfection of cellulose IV_I depends on the crystallinity of the original material: either of the starting cellulose I or of the cellulose III_I after ammonia treatment. The product thus obtained was analogous to cellulose I_β, which is what it should be called rather than cellulose IV_I. If the existence of the polymorph cellulose IV_I is not accepted, the observations on which it has been based may be explained by the fact that the structure termed cellulose IV_I is cellulose I_β which contains lateral disorder.

Introduction

It had long been believed that native cellulose was a unique structure called cellulose I. In 1984, however, Atalla and VanderHart[1,2] proposed from high-resolution ^{13}C CP/MAS NMR spectra that native celluloses consisted of two distinct crystalline allomorphs, namely cellulose I_α and I_β. Later the structures of these polymorphs were revealed by microdiffraction.[3] Cellulose I_α has a triclinic one-chain unit cell where parallel cellulose chains stack, via van der Waals interactions, with progressive shear parallel to the chain axis. Cellulose I_β has a monoclinc two-chain unit cell, which means parallel cellulose chains stacked with alternating shear. Furthermore, it has been shown that I_α entirely transforms into I_β without losing its crystallinity, by hydrothermal treatment[4−6] or by treatments with various solvents.[7]

Cellulose II is another cellulose polymorph, which results from the treatment of cellulose I by alkali solution, mercerization, or recrystallization from a solution. The structure of cellulose II is believed to consist of a two chain $P2_1$ monoclinic unit cell where cellulose chains are stacked with opposite polarity, a so-called antiparallel structure.[8−10]

Another polymorph, cellulose III_I, is obtained by treatment of cellulose I in liquid ammonia[11,12] or various amines[13−15] followed by the removal of these reagents. Yatsu et al.[16] developed a treatment in super-critical ammonia fluid for preparing highly crystalline cellulose III_I. X-ray diffraction studies, using the highly crystalline samples thus prepared, revealed that the structure of cellulose III_I is a monoclinic one chain unit cell with $P2_1$ symmetry, indicating parallel cellulose chains stacked with no stagger along the chain axis.[17]

Hutino and Sakurada defined cellulose IV as an another polymorph of cellulose by the X-ray diffraction method in 1940.[18] Whereas the typical two equatorial reflections of cellulose I appeared at about 0.6 and 0.5 nm, the corresponding reflection of cellulose IV was positioned between those two reflections. A detailed review concerning preparation methods and final products of this polymorph was reported by Kulshreshtha.[19] In general, cellulose IV could be prepared by treatment in glycerol at 260 °C after transformation into cellulose II or III.[20] Cellulose I cannot be transformed directly into cellulose IV.

Why is it necessary to convert cellulose I to cellulose III_I before transforming into cellulose IV_I? It may be that fibrillation of cellulose microfibrils, which makes them more accessible to the reaction for transformation to cellulose IV_I, occurred through the change to cellulose III_I.[21,22] However, the fibrillation makes cellulose IV_I less suitable for crystallographic analysis: that is, it makes it more difficult to interpret cellulose IV_I as a crystal. For these reasons, the issue about cellulose IV_I, whether it is a crystal with an orthogonal unit cell[23] or a less crystalline form of cellulose I,[24,25] is still debated.

In this study, therefore, we tried to monitor the I → III_I → IV_I transformation, maintaining the crystallinity of the

* To whom correspondence should be addressed. Phone: +81-3-5841-5247. Fax: +81-3-5684-0299. E-mail: wadam@sbp.fp.a.u-tokyo.ac.jp.
† The University of Tokyo.
‡ Centre de Recherches sur les Macromolécules Végétales.
§ Kyoto University.

10.1021/bm0345357 CCC: $27.50
Published on Web 05/14/2004

original sample by X-ray diffraction, FT-IR, and solid-state ^{13}C NMR spectroscopy. By comparing the transformation behavior of a highly crystalline, I_α rich type algal cellulose and ramie fiber cellulose of the I_β type, we reinvestigated the cellulose IV_I structure.

Experimental Section

Cellulose Samples. The green alga *Cladophora* sp. was harvested from the sea of Chikura, Chiba, Japan. The whole plants were immersed overnight in 5% KOH at room temperature. After thoroughly washing in water, they were then purified by bleaching in 0.3% $NaClO_2$ at 70 °C for 3 h. These treatments were repeated several times until the sample became perfectly white.[26] The purified cell wall was homogenized into small fragments using a double-cylinder type homogenizer and dried by lyophilization. The powder samples thus obtained were stored in a desiccator until used.

Purified samples before drying were treated with 50% sulfuric acid at 70 °C for 8 h with continuous stirring. The samples were then washed with deionized water by successive dilution and centrifugation at 3200 *g* for 5 min until the supernatant became turbid. The suspension was concentrated by high-speed centrifugation at 18 800 *g* for 40 min and then dispersed in a small amount of distilled water. The concentrated suspension was sonicated with a rod type sonicator for 1 min.

The suspension was cast on a glass plate and dried in air for a few days. The cast films with random orientation were further dried at 105 °C for 8 h and stored in a desiccator until used.

Oriented films of cellulose microcrystals were prepared according to the method described in our previous paper.[27] In short, the suspension with a small amount of sulfuric acid was put into a glass vial, and the vial was then kept horizontal and rotated around its center. After a few hours, the gel layer attached to the inner surface of the glass vial was dried into a film by repeatedly rinsing with ethanol and drying with a warm airflow. The films of oriented microcrystals were further dried at 105 °C for 8 h and stored in a desiccator until used.

A bast fiber ramie was also used. The fiber was repeatedly purified with 5% KOH and 0.3% $NaClO_2$ solution as above. The purified fiber was air-dried, further dried at 105 °C for 8 h, and stored in a desiccator until used.

Hydrothermal Treatment. The films were inserted into a steel pressure vessel with a 0.1 N NaOH solution. The vessel was sealed and then heated in an oil bath to 260 °C. After holding at the temperature for 0.5 h, the vessel was cooled under tap water.[5,6] The treated films were thoroughly washed in a large amount of deionized water and then dried at 105 °C overnight.

Super-Critical Ammonia Treatment. The films were inserted into a steel pressure vessel, which was cooled in a dry ice and methanol bath. The NH_3 gas was introduced into the cooled vessel, and the sample was immersed in liquid NH_3. The vessel was hermetically sealed and maintained at room temperature for 30 min. The vessel was heated in an oil bath at 140 °C (a few degrees over the critical temperature of ammonia, i.e., 132.5 °C) for 1 h and the NH_3 gas was leaked from the vessel after removing it from the oil bath.[16,17,28] The treated samples were washed with dry methanol and dried under high vacuum at 50 °C.

Conventional Liquid Ammonia Treatment. The films were treated in an ampule of liquid ammonia cooled in a bath of dry ice and methanol mixture. After 3 h of immersion, the samples were removed and dried at room temperature under strong ventilation. The dried samples were further dried under high vacuum at room temperature.

Glycerol Treatment. The ammonia treated samples were first soaked in glycerol for 3 days at room temperature, replacing the glycerol every day. The samples in glycerol were put into the steel pressure vessel, and a small amount of fresh glycerol was also added. The vessel was sealed and heated in an oil bath to 260 °C.[20,23] After 0.5 h, the vessel was cooled under tap water. The product was washed successively with water and acetone and dried under high vacuum at 50 °C.

X-ray Diffraction. X-ray fiber diagrams were obtained using a vacuum camera mounted on a Rigaku RU-200BH rotating anode X-ray generator. Ni-filtered Cu Kα radiation ($\lambda = 0.15418$ nm) generated at 50 kV and 100 mA was collimated by a pinhole 0.3 mm diameter. X-ray diffraction patterns were recorded on Fuji Imaging Plates (BAS−IP SR 127), and the camera length was calibrated using NaF ($d = 0.23166$ nm).

Equatorial profiles in 2θ range of 10−30° were obtained from the diffraction images by using software Rigaku R-axis. Peak separations of the profiles were carried out using a least-squares fitting method, where a pseudo-voight function for each crystalline peak and fifth-degree polynomial function for the background were used as described in previous papers.[29,30] The crystallinity index (CrI) was determined from the ratio of the separated peak area to the total area. The crystallite sizes of the direction perpendicular to the most condensed plane, which correspond to the direction [100] of cellulose I_β were calculated using the Scherrer equation as previously reported. [29, 30]

FT-IR Spectroscopy. Randomly oriented thin films were used. FT-IR spectra were obtained with a Nicolet Magna 860. The wavenumber range scanned was 4000−400 cm^{-1}; 64 scans of 4 cm^{-1} resolution were signal-averaged and stored.

Solid-State ^{13}C NMR Spectroscopy. Freeze-dried samples were used for the NMR experiments. They were performed with a Bruker MSL spectrometer operated at a ^{13}C frequency of 25 MHz, using the combined techniques of proton dipolar decoupling (DD), magic angle spinning (MAS), and cross-polarization (CP). ^{13}C and ^{1}H field strengths of 64 kHz corresponding to 90° pulses of 4 ms were used for the matched spin-lock cross-polarization transfer. The spinning speed was set at 3000 Hz. The contact time was 1 ms, the acquisition time 70 ms, the frequency width 29 400 Hz and the recycling delay 4 s. A typical number of 10 000 scans were acquired for each spectrum. Chemical shifts were referred to tetramethylsilane after calibration with the carbonyl signal of glycine at 176.03 ppm.

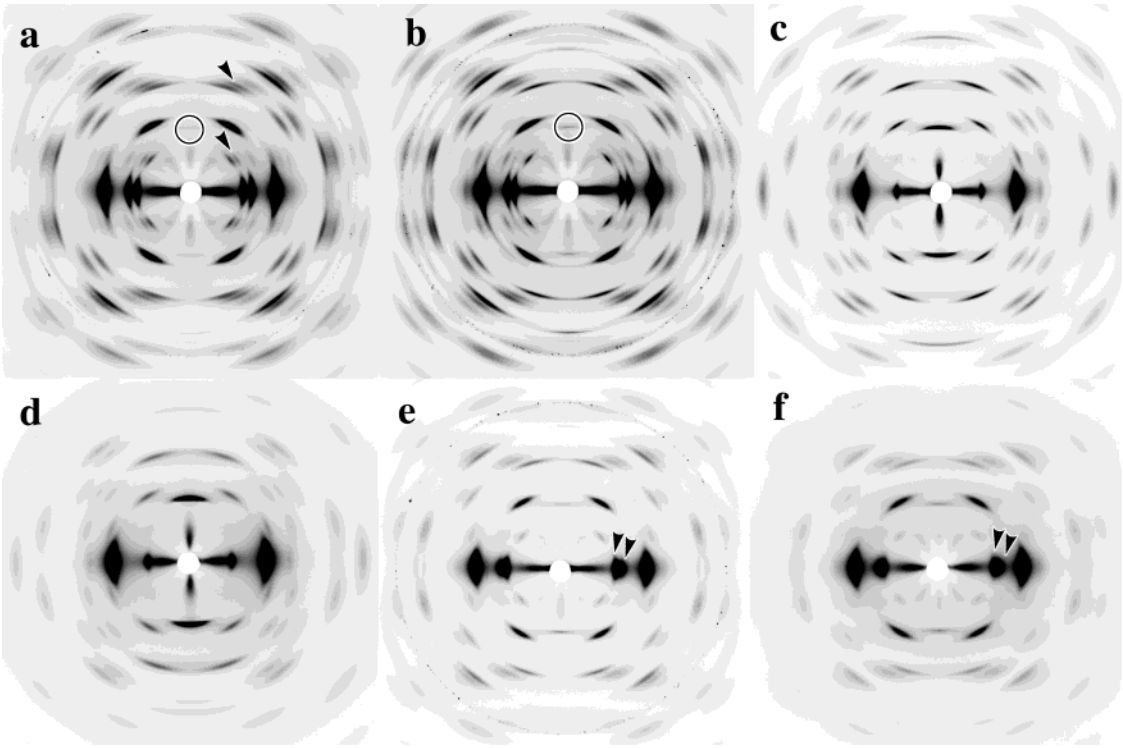

Figure 1. X-ray fiber diffraction diagrams obtained from uniaxial oriented *Cladophora* cellulose films: (a) initial cellulose, (b) hydrothermally treated cellulose, (c) super-critical ammonia treated cellulose, (d) liquid ammonia treated cellulose, (e) super-critical ammonia treated followed by glycerol treated cellulose, and (f) liquid ammonia treated followed by glycerol treated cellulose. Arrowheads in part a indicate reflections originating from I_α phase. Those reflections are missing in part b, and circled reflections corresponding to I_β 002 are enhanced by the hydrothermal treatment, which causes I_α to I_β conversion. Two reflections indicated by arrowheads in parts e and f correspond to I_β $1\bar{1}0$ and 110, which show that the cellulose III_I was transformed into cellulose I_β by the glycerol treatment.

Results and Discussion

X-ray Diffraction. Figure 1 shows X-ray fiber diffraction diagrams of *Cladophora* polymorphs examined in this study.

The fiber diagram of the initial cellulose (a) is a well-resolved pattern of the I_α rich type of cellulose: 70% I_α phase and 30% I_β phase.[29] On the other hand, that of cellulose treated in 0.1 N NaOH solution at 260 °C for 30 min (b) is a typical pattern of converted I_β cellulose. Both diagrams were very similar, but some diffraction spots that did not exist in (b) were observed in (a). Those spots indicated by arrowheads, which were in the first and third layer lines, were attributed to the I_α phase. After the hydrothermal treatment, these spots disappeared and some characteristic I_β reflections, for instance the 002 meridional reflection (circled), were enhanced, indicating that I_α transformed into I_β by this treatment.[6]

Two cellulose III_I samples were obtained by treating *Cladophora* cellulose either in supercritical ammonia fluid or in cold liquid ammonia. Both diagrams (c and d) indicated that cellulose I had been completely transformed into III_I. The diagram from the supercritical ammonia treated sample (c) was slightly better organized in the higher layer lines implying a more highly crystalline state.

During the conversion cellulose I $\rightarrow$ III_I, the crystal lattice undergoes rapid swelling and deswelling, and the resulting volume change exceeds the limit of elasticity of cellulose crystallites. As a result, the formation of cracks perpendicular to the direction of swelling, i.e., cracks along the chain direction, has frequently been observed.[21,31] This phenomenon was more evident when we used the conventional ammonia treatment.

Fiber diagrams (e) and (f) were recorded from the samples (c and d) treated in glycerol at 260 °C for 30 min. It had been reported that cellulose III_I with normal crystallinity was converted into cellulose IV_I by glycerol treatment.[23] From these samples, therefore, we expected that highly crystalline cellulose IV_I would be produced. However, the recorded patterns (e and f) were somewhat different from previously reported cellulose IV_I,[23] because two independent reflections, indicated by arrowheads, were noticeable. In the case of cellulose IV_I, these two peaks should appear as a single peak.[23] Although different from the diagram of cellulose IV_I, the patterns (e and f) were similar to the pattern (b) of the I_β phase. This result indicates that cellulose III_I was transformed into cellulose I_β by the glycerol treatment, in agreement with the consequence of simple heating of cellulose III_I.[32] Although several times we tried repeating glycerol treatments at a higher temperature, only the cellulose I_β pattern was obtained in all cases. The difference between (e) and (f) was also noticeable. The diagram (e) showed better resolution, probably because of the greater perfection of the corresponding cellulose III_I structure.

Figure 2 shows equatorial diffraction profiles of hydrothermally (a), super-critical ammonia followed by glycerol (b), and liquid ammonia followed by glycerol (c) treated *Cladophora* celluloses, which were obtained from fiber diffraction diagrams of Figure 1, parts b, e, and f, respec-

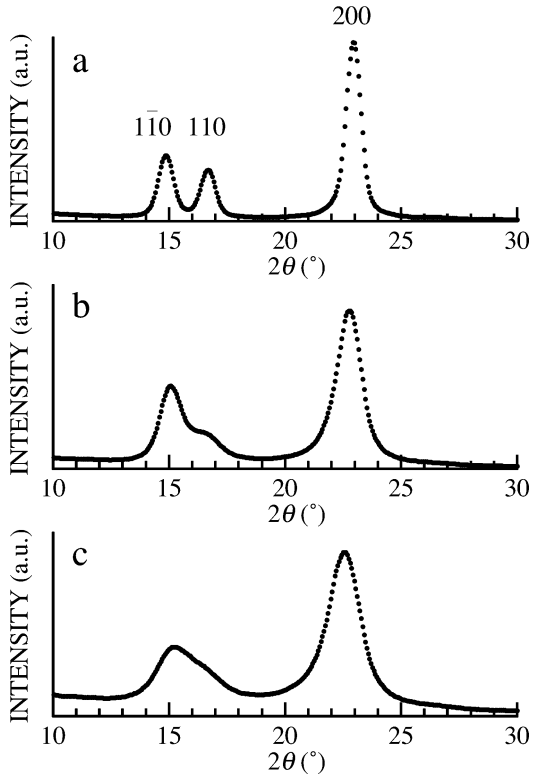

Figure 2. Equatorial X-ray diffraction profiles of (a) hydrothermally treated, (b) super-critical ammonia treated followed by glycerol treated, and (c) liquid ammonia treated followed by glycerol treated *Cladophora* celluloses, obtained from fiber diffraction diagrams of Figure 1, parts b, e, and f, respectively.

Table 1. *d* Spacings, Crystallite Sizes, and Crystallinity Indices of the *Cladophora* Samples

	d-spacings (nm)[a]				
Cladophora cellulose	(1$\bar{1}$0)	(110)	(200)	*L* (nm)[b]	CrI[c]
hydrothermally treated	0.596	0.532	0.388	10.5	0.79
super-critical ammonia and glycerol treated	0.589	0.539	0.391	6.2	0.73
liquid ammonia and glycerol treated	0.585	0.539	0.395	4.9	0.60

[a] *d* spacings of typical three equatorial peaks of cellulose I_β. [b] Crytalllite size of the direction [100] of cellulose I_β. [c] Crytallinity index.

tively. *d*-Spacings corresponding to three equatorial peaks of cellulose I_β, crystallite sizes, and crystallinity indices calculated from those profiles are also listed in Table 1. The smaller the size and/or the crystallinity index is, the peak positions of 1$\bar{1}$0 and 110 diffraction comes closer, which allows us to imagine that those two peaks would merge into a single peak for the lower crystalline cellulose. How about the ramie cellulose?

X-ray diffraction diagrams of ramie polymorphs are shown in Figure 3: initial (a), supercritical ammonia (b), and cold ammonia (c) further glycerol treated cellulose samples. The initial ramie cellulose (a) was I_β, but the crystallinity was much less than in the hydrothermally treated *Cladophora* cellulose (Figure 1b). The fiber diagram (b) of the cellulose prepared using supercritical ammonia and subsequent glycerol treatment differed from the previously reported cellulose IV_I pattern.[23] In that, the two reflections assigned to I_β 1$\bar{1}$0 and 110 were nearly merged but still resolved. On the other hand, the fiber diagram (c) prepared by the low temperature ammonia and subsequent glycerol treatment was identical with the previously reported cellulose IV_I pattern.[23] Two equatorial peaks overlap to appear as one single peak. It was also observed that the intensity of the circled 002 reflection was slightly increased by this treatment.[33]

In our previous paper,[34] we reported that the two I_β reflections, 1$\bar{1}$0 and 110, became closer with a decrease of the cellulose crystallite size and crystallinity. As the crystallite size of ramie was smaller than the hydrothermally treated *Cladophora* cellulose, the distance between the two reflections in the former cellulose was less than that of the latter. From the results using cellulose of large crystallite size (Figure 1), the ammonia with further glycerol treatment was found to be a method for reducing the crystallite size and crystallinity but not a method for preparing the cellulose IV_I allomorph. The two overlapping reflections in diagram (c) would then arise because cellulose crystallites much smaller than ramie cellulose microfibrils were prepared by the treatment. It might be possible to calculate atomic coordinates on the assumption that cellulose IV_I is a crystal with an orthorhombic unit cell. However, the actual form of cellulose IV_I should be described as cellulose I_β whose crystallite size is fairly small; it is not a distinct polymorph of cellulose.

To summarize, the perfection of cellulose IV_I depends on the crystallinity of the original sample; either the starting cellulose I or the cellulose III_I after ammonia treatment. The products thus obtained were analogous to cellulose I_β having

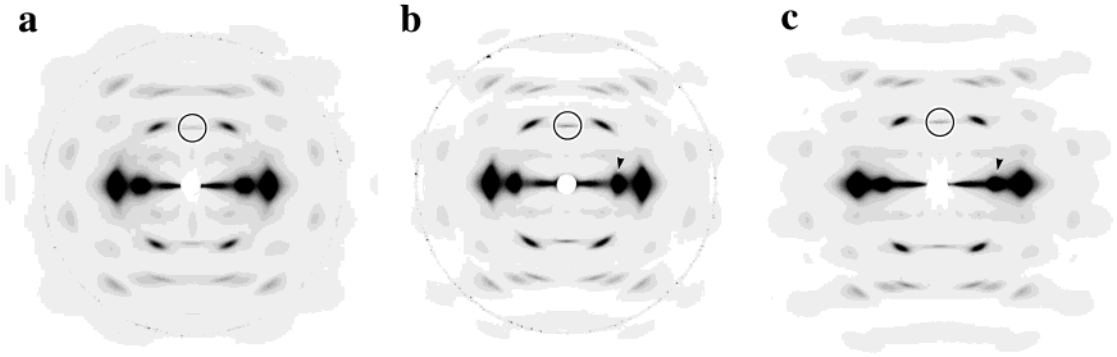

Figure 3. X-ray fiber diffraction diagrams of ramie cellulose: (a) initial, (b) super-critical and further ammonia treated cellulose, and (c) liquid ammonia and further glycerol treated cellulose. Arrowheads in parts b and c show overlapping of I_β 1$\bar{1}$0 and 110 reflections. The circled 002 reflection is slightly intensified by the treatment.

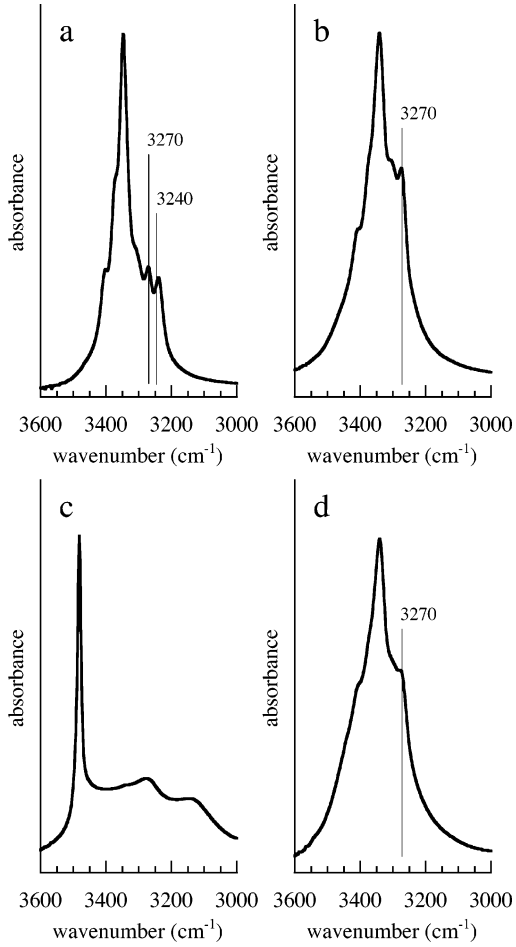

Figure 4. FT-IR spectra of highly crystalline *Cladophora* cellulose in the OH stretching regions: (a) initial cellulose, (b) hydrothermally treated cellulose, (c) super-critical ammonia treated cellulose, and (d) super-critical ammonia and further glycerol treated cellulose. Bands at 3240 and 3270 cm^{-1} are assigned to the I_α and I_β phases, respectively.[26]

various degrees of lateral disorder, which is what they should be called rather than cellulose IV_I.

For further spectroscopic analysis, we focused on the cellulose IV_I samples prepared via cellulose III_I obtained after supercritical ammonia treatment, because the signals were much sharper and there were no substantial difference from the cellulose IV_I sample prepared via cellulose III_I obtained by low-temperature ammonia treatment.

FT-IR Spectroscopy. Structural differences among cellulose polymorphs were characterized as differences in the hydrogen bonding pattern. FT-IR measurements were carried out for variously treated cellulose thin films. Figure 4 shows FT-IR spectra of the OH stretching region for *Cladophora* celluloses: initial (a), hydrothermally treated (b), super-critical ammonia treated (c), and ammonia and further glycerol treated (d) celluloses.

Although the absorption band at 3240 cm^{-1} assigned to I_α existed in the initial spectrum (a) of *Cladophora* cellulose containing 70% I_α, it did not exist in the spectrum (b) of the hydrothermally treated cellulose. On the contrary, the absorbance of the characteristic I_β band at 3270 cm^{-1} in (b) was about two times stronger than the corresponding band in (a). These results indicate that I_α was transformed into I_β by the hydrothermal treatment.

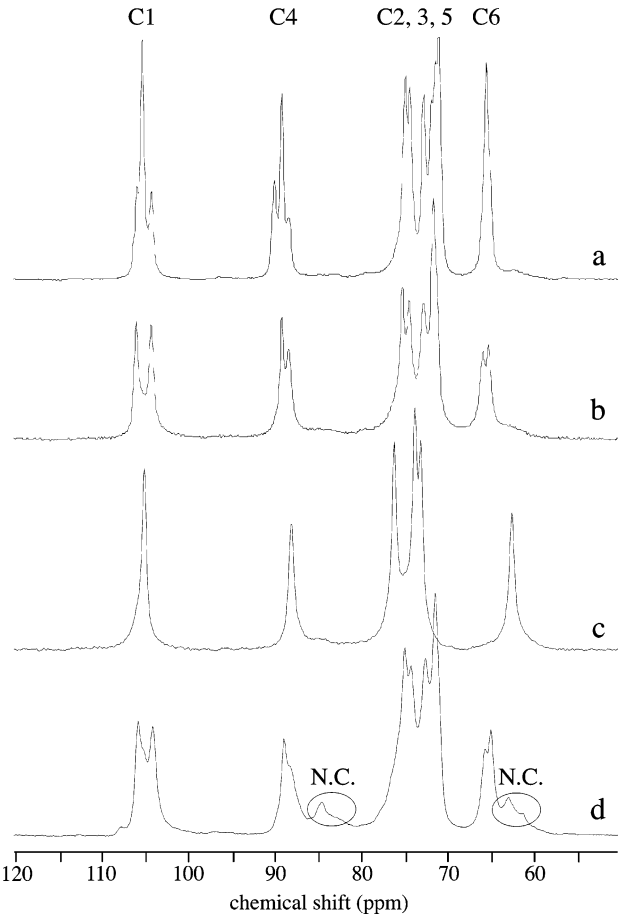

Figure 5. Solid-state ^{13}C NMR spectra of *Cladophora* celluloses; parts a−d are same as Figure 4.

In the spectrum of cellulose III_I (c), only three bands existed: one sharp band at 3480 cm^{-1} and two further broad bands at 3300 and 3150 cm^{-1}. This spectrum was different from the complicated spectrum of cellulose I, indicating that cellulose I was completely converted into cellulose III_I without any remaining.

The spectrum (d) of the cellulose III_I sample treated in glycerol at 260 °C for 30 min was almost the same as the spectrum (b) of cellulose I_β, except that it was less resolved. Therefore, we consider that the glycerol treatment is a method to convert cellulose III_I to I_β. Regarding to the lower crystalline celluloses, Marrinan and Mann already reported that the spectrum of cellulose IV_I is very similar to that of original ramie cellulose.[35] This study does not contradict our FT-IR study using highly crystalline *Cladophora* celluloses.

Solid-State ^{13}C NMR Spectroscopy. Solid-state ^{13}C NMR spectra of *Cladophora* celluloses without any mathematical resolution enhancement are shown in Figure 5: initial (a), hydrothermally treated (b), super-critical ammonia treated (c), and ammonia and further glycerol treated (d) celluloses. Crystallinity indices and I_β contents of the samples were determined from the spectra and are listed in Table 2.

The NMR spectrum of initial *Cladophora* cellulose (a) is a spectrum typical of I_α rich type celluloses such as those of *Valonia* and bacterial celluloses. The spectrum of hydrothermally treated cellulose (b) is that of cellulose I_β. This is due to the fact that the I_α was transformed into I_β by the treatment. When *Cladophora* cellulose was treated with

Table 2. Crystallinity Indices and I_β Contents of the *Cladophora* and Ramie Samples

		CrI[a]	I_β content[b]
Cladophora	initial	0.93	0.46
	hydrothermally treated	0.87	0.92
	ammonia treated	0.74	ND
	ammonia and glycerol treated	0.65	more than 0.99
ramie	initial	0.67	0.90
	ammonia and glycerol treated	0.52	more than 0.99

[a] Crystallinity index determined as the ratio from C4 crystalline area over total C4 area. [b] I_β content determined with the peaks attributed to C4.

super-critical ammonia, another polymorph, cellulose III_I, was obtained. The spectrum (c) is characteristic of cellulose III_I in exhibiting only six peaks corresponding to the six carbon atoms. It was believed for a long time that cellulose III_I was converted into cellulose IV_I by glycerol treatment. However, the spectrum (d) was nearly identical to the spectrum (b) of cellulose I_β. This result indicated that the cellulose III_I was transformed into cellulose I_β by the glycerol treatment at 260 °C, in good agreement with the results of the X-ray diffraction and FT-IR experiments mentioned above. It has been known that heating the sample in water or in an inert atmosphere can transform cellulose III_I into I_β.[21,22,32] Considering the similarity between these treatments and the glycerol treatment, the essential factor in transforming cellulose III_I into I_β must be the high temperature.

From the position of the C6 resonance of the spectra, we can judge the conformation of hydroxymethyl group of each cellulose polymorph.[36] The spectra indicated that both cellulose I_α and I_β had the *tg* conformation, but cellulose III_I had the *gt* conformation suggesting a lack of O6−O2 intramolecular hydrogen bonding.[37] Thus, the conformation was returned back to the *tg* (i.e., cellulose I type) conformation by the glycerol treatment of cellulose III_I. This result indicates that the intramolecular hydrogen bonding was reversible during transformations among the cellulose I family: I_α, I_β, and III_I polymorphs. However, the broad lines at about 85 and 63 ppm, which correspond respectively to C4 and C6 noncrystalline resonances, increased in relative intensity. These resonances may arise from the newly produced surface of the crystallites,[38] because fibrillation that occurred when cellulose III_I was converted to I_β by the treatment.[21,22] In addition, as shown in Table 2, the crystallinity index of the glycerol treated sample, cellulose IV_I, was fairly low. On this basis, cellulose IV_I would be explained as a laterally disordered cellulose I_β structure whose crystallites were small.

Solid-state ^{13}C NMR spectra of ramie celluloses are shown in Figure 6: initial (a) and ammonia and further glycerol treated (b) celluloses. Spectra a and b were obtained from samples whose crystal forms were assigned as cellulose I_β and IV_I, respectively, from the above X-ray diffraction results. However, taking into account the agreement with results from highly crystalline *Cladophora* cellulose, it seemed likely that ramie cellulose treated with ammonia and then glycerol is more disordered form of cellulose I_β than similarly treated *Cladophora* cellulose.

Why Cellulose III_I as Intermediate? To prepare cellulose IV_I, why is it necessary to pass through cellulose III_I? Why does glycerol treatment not transform cellulose I directly into cellulose IV_I? Debzi et al.[7] reported that the glycerol treatment was able to transform cellulose I_α to I_β, so the treatment does not cause the breakdown of O6−O2 hydrogen bonding. Thus, the *tg* conformation of the hydroxylmethyl group of cellulose I is stable, remaining *tg* after the treatment.[37] On the contrary, the ^{13}C NMR spectrum of cellulose III_I indicated that the conformation of the hydroxylmethyl group was *gt*, which suggested that O6−O2 hydrogen bonding was absent.[17,37] Due to the absence of the hydrogen bonding, the flexibility of the chains increased and the lateral order of the crystallite was eventually lost. As reported by Chanzy et al.,[39,40] cellulose IV_I found in the cellulose of a primary wall, would be a structural form where the order of chain direction was retained but the structure was paracrystalline, disordered in a lateral direction. From the results of diffraction and FT-IR methods, the structure is quite similar to cellulose I_β, in correspondence with the low crystalline cellulose observed in fungal cell walls.[41]

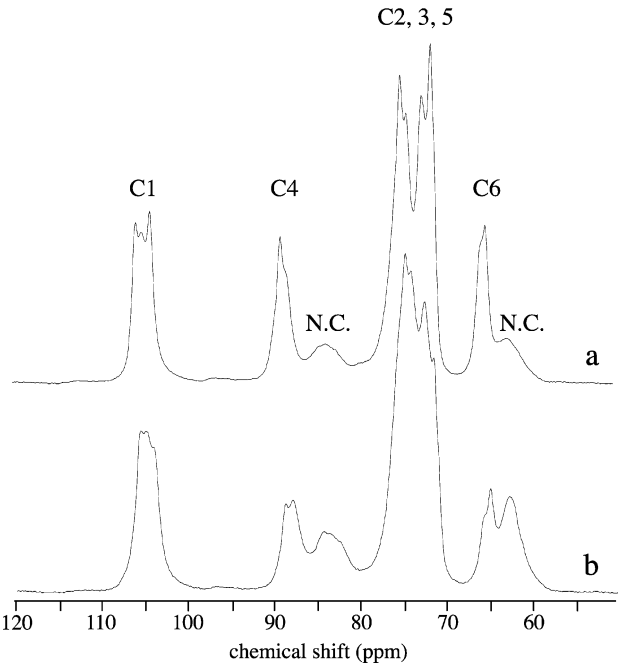

Figure 6. Solid-state ^{13}C NMR spectra of ramie celluloses; parts a and b are the same as Figure 2.

Acknowledgment. This work was partly supported by the Grant-in-Aid for Scientific Research from the Ministry of Education, Science, Sports and Culture, Japan (Grant No. 10760105). The help of Dr. Jarvis, Glasgow University, with the language and discussion is gratefully acknowledged.

References and Notes

(1) Atalla, R. H.; VanderHart, D. L. *Science* **1984**, *223*, 283−285.
(2) VanderHart, D. L.; Atalla, R. H. *Macromolecules* **1984**, *17*, 1465−1972.
(3) Sugiyama, J.; Vuong, R.; Chanzy, H. *Macromolecules* **1991**, *24*, 4168−4175.
(4) Horii, F.; Yamamoto, H.; Kitamaru, R.; Tanahashi, M.; Higuchi, T. *Macromolecules* **1987**, *20*, 2946−2949.
(5) Yamamoto, H.; Horii, F.; Odani, H. *Macromolecules* **1989**, *22*, 4130−4132.
(6) Sugiyama, J.; Okano, T.; Yamamoto, H.; Horii, F. *Macromolecules* **1990**, *23*, 3196−3198.
(7) Debzi, E. M.; Chanzy, H.; Sugiyama, J.; Tekely, P.; Excoffier, G. *Macromolecules* **1991**, *24*, 6816−6822.

(8) Stipanovic, A.; Sarko, A. *Macromolecules* **1976**, *9*, 851.
(9) Kolpak, K.; Blackwell, J. *Macromolecules* **1976**, *9*, 273.
(10) Langan, P.; Nishiyama, Y.; Chanzy, H. *J. Am. Chem. Soc.* **1999**, *121*, 9940−9946.
(11) Hess, K.; Trogus, C. *Chem. Ber.* **1935**, *68*, 1986−1988.
(12) Barry, A. J.; Preston, F. C.; King, A. J. *J. Am. Chem. Soc.* **1936**, *58*, 333−337.
(13) Trogus, C.; Hess, K. *Z. Phys. Chem. (Leipzig)* **1931**, *B14*, 387−395.
(14) Davis, W. E.; Barry, A. J.; Preston, F. C.; King, A. J. *J. Am. Chem. Soc.* **1943**, *65*, 1294−1299.
(15) Sarko, A.; Southwick, J.; Hayashi, J. *Macromolecules* **1976**, *9*, 857−863.
(16) Yatsu, L. Y.; Calamari, T. A., Jr; Benerito, R. R. *Text. Res. J.* **1986**, *56*, 419−424.
(17) Wada, M.; Heux, L.; Isogai, A.; Nishiyama, Y.; Chanzy, H.; Sugiyama, J. *Macromolecules* **2001**, *34*, 1237−1243.
(18) Hutino, k.; Sakurada, I. *Naturwissenschaften* **1940**, *28*, 577−578.
(19) Kulshreshtha, A. K. *J. Text. Inst.* **1979**, *1*, 13−18.
(20) Loeb, L.; Segal, L. *J. Polym. Sci.* **1954**, *14*, 121−123.
(21) Roche, H.; Chanzy, H. *Int. J. Biol. Macromol.* **1981**, *3*, 201−206.
(22) Chanzy, H.; Henrissat, B.; Vincendon, M.; Tanner, S. F.; Belton, P. S. *Carbohydr. Res.* **1987**, *160*, 1−11.
(23) Gardiner, E. S.; Sarko, A. *Can. J. Chem.* **1985**, *63*, 173−180.
(24) Howsmon, J. A.; Sisson, W. A. In *Cellulose and Cellulose Derivatives*, 2nd ed.; Ott, E., Ed.; Interscience: New York, 1954; pp 231−346.
(25) Marrinan, H. J.; Mann, J. *J. Polym. Sci.* **1956**, *31*, 301−311.
(26) Sugiyama, J.; Persson, J.; Chanzy, H. *Macromolecules* **1991**, *24*, 2461−2466.
(27) Nishiyama, Y.; Kuga, S.; Wada, M.; Okano, T. *Macromolecules* **1997**, *30*, 6395−6397.
(28) Isogai, A.; Usuda, M.; Kato, T.; Uryu, T.; Atalla, R. H. *Macromolecules* **1989**, *22*, 3168−3172.
(29) Wada, M.; Okano, T.; Sugiyama, J. *Cellulose* **1997**, *4*, 221−232.
(30) Wada, M.; Okano, T. *Cellulose* **2001**, *8*, 183−188.
(31) Sugiyama, J.; Harada, H.; Saiki. H. *Int. J. Biol. Macromol.* **1987**, *9*, 121−129.
(32) Wada, M. *Macromolecules* **2001**, *34*, 3271−3275.
(33) Hayashi, J.; Sueoka, A.; Ookita, J.; Watanabe, S. *Nippon Kagaku Kaishi* **1973**, *3*, 146−152.
(34) Wada, M.; Sugiyama, J.; Okano, T. *Mokuzai Gakkaishi* **1994**, *40*, 50−56.
(35) Marrinan, H. J.; Mann, J. *J. Polym. Sci.* **1956**, *21*, 301−311.
(36) Horii, F.; Hirai, A.; Kitamaru, R. In *The structure of cellulose; Characterization of the solid states*; Atalla, R. H., Ed.; ACS Symposium Series 340; American Chemical Society: Washington, DC, 1987; Chapter 6, pp 119−134.
(37) The conformation of the hydroxymethyl group is defined by two letters, the first referring to the torsion angle χ (O5−C5−C6−O6) and the second to the torsion angle χ' (C4−C5−C6−O6). Thus the ideal *tg* and *gt* conformations would respectively be defined as sets of two angles (180°, 60°) and (60°, 180°).
(38) Viëtor, R. J.; Newman, R. H.; Ha, M. A.; Apperley, D. C.; Jarvis, M. C. *Plant J.* **2002**, *30*, 721−731.
(39) Chanzy, H.; Imada, K.; Vuong, R. *Protoplasma* **1978**, *94*, 299−306.
(40) Chanzy, H.; Imada, K.; Mollard, A.; Vuong, R.; Barnoud, F. *Protoplasma* **1979**, *100*, 303−316.
(41) Helbert, W.; Sugiyama, J.; Ishihara, M.; Yamanaka, S. *J. Biotech.* **1997**, *57*, 29−37.

BM0345357